Los Alamos National Laboratory is operated by the University of California for the United States Department of Energy under contract W-7405-ENG-36

LA-UR--87-3171

DE88 000491

TITLE RESPONSE OF PROPELLANTS TO HYPERVELOCITY ATTACK

AUTHOR(S) B. W Asay, J. B. Ramsay, and A. W. Campbell
Los Alamos National Laboratory, M-8

SUBMITTED TO DEA Proceedings, MBB Schrobenhausen, Germany, July 1987

DISCLAIMER

Los Alamos Los Alamos National Laboratory
Los Alamos, New Mexico 87545

RESPONSE OF PROPELLANT TO HYPERVELOCITY ATTACK

Blaine W Asay, John B. Ramsay, and A. Wayne Campbell
Explosives Applications Group, M-8
Los Alamos National Laboratory
P.O. Box 1663, MS J960
Los Alamos, NM 87545

This study was undertaken to examine the behavior of heterogeneous gun propellants when they are impacted by shaped-charge jets. In the immediate area surrounding the impact point, the pressure is believed to be above the detonation pressure of the full-density propellant. However, a detonation does not necessarily occur, and if it does, the detonation does not necessarily propagate. This is a function of grain size, web, perf pattern, jet diameter, propellant failure diameter, and composition. We hope to eventually understand the mechanism and physics of the failure of detonation in these systems. This report summarizes the initial work performed in support of the study. The results presented here formed the groundwork for a more specific effort, which is continuing.

Figure 1 is a schematic description of the model we are using to help define the regions of interest in the case of detonation failure. The jet impacts the propellant and initiates a detonation in the immediate vicinity of the jet tip. Detonation proceeds for a certain distance and a transition to a violent deflagration occurs. This reaction propagates until a transition to a mild burn occurs. The delineation between these regions may or may not be clear-cut and this description is necessarily, in the absence of experimental evidence, overly simplified. However, the ideas are conceptually sound, and it is with this model in mind that the initial experimental plan was devised.

We first performed several tests that were intended to provide experience with the new materials. These were followed by a series of tests in which radiographs were taken of the reaction front at different times to determine if the reaction front structure and detonation failure could be identified. Several shots using shock pins on the outside of the containment vessel to measure wave velocities were then fired. The tests to this point used a booster of PBX 9501 (95% HMX, 5% Estane) at the top of a confining tube to initiate the reaction in the propellant bed. Finally, two tests were conducted in which small shaped-charge jets were fired into a bed of propellant. These tests will be described in

turn. Table I shows the composition of the gun propellant that was used throughout this series of tests.

Reaction Front Visualization

The propellant was confined in polymethylmethacrylate (PMMA) tubes 2.5-in. o.d., 2.0-in. i.d. and 6 in. long. The tube containing the propellant was placed on an 8-by 8-by 3-in.-thick steel witness plate. Radiographs (450 keV) were taken of the reaction front at various times. PBX 9501 (2-in. diam. by 2-in. long right circular cylinder) was used to initiate the reaction. Figures 2-7 are prints of the radiographs obtained during this portion of the study. Each radiograph represents a separate test with conditions identical to the others in this series. Only the time at which the radiograph was taken was varied. The reaction front is fairly thin and well-defined immediately after initiation. It becomes more diffuse as time progresses. Examination of the witness plate after each of the tests revealed no dent. The only markings on the plate were an occasional small indentation that most likely occurred when a reacting pellet was driven into the plate.

The position of the reaction front was obtained visually and plotted against time. This plot is shown in Figure 8. Note here (it will be demonstrated later) that a constant velocity detonation was never achieved.

One other test was carried out in this series in which a PMMA tube described above was packed with propellant. Three individual grains of propellant were wrapped in a 1-mil (0.25-μm) lead foil and these were placed into the bed at three locations. The bed was initiated as described above and two radiographs were taken at separate times. Figures 9 (a) and (b) show radiographs of the bed before initiation. The two views are the result of using two x-ray tubes positioned at different angles. Figures 10 (a) and (b) show the tube at two distinct times after initiation. Two observations can be made. First, no significant compression of the bed is evident ahead of the main reaction front. The reaction front is almost touching the tracer particle in Figure 10 (a), but the particle has not moved or been deformed. Second, complete reaction is seen to occur, but no clearly defined thin reaction front exists, as is observed in a detonation.

Instrumented Pin Tests

Figure 11 is a schematic of the test configuration that was used during this portion of the study. Three different tubes were used, all 12 in. long. Two were copper of 1.87-in. i.d. and 3.37-in. i.d. respectively. Each had 1/16-in. wall thickness. The third tube was PMMA, 2.5-in. o.d. and 2.0-in. i.d. The brass shock pins were offset from the tube by a thin

Mylar tape. In the test using the PMMA tube, a thin copper foil was glued to the wall to provide the conduction plane required. A foil switch was placed between the tube and the witness plate to record overall transit times.

Figure 12 shows the shock pin data for the 1.87-in. i.d. copper tube. The slope of the least-squares line is 3.3 mm/μs. Figure 13 shows the pin data for the 3.37-in. copper tube. The slope was 4.4 mm/μs. In both these tests, as shown by the shock pin data, a steady velocity was obtained. Figure 14 shows the data taken when the propellant confined in the PMMA tube was initiated. A steady velocity was never established.

To ensure that the copper tubes were long enough to allow failure, two more shots were fired in which the tube lengths were increased to about 10 diameters. That is, the 1.87-in. i.d. copper tube length was increased to 20 in. and the 3.37-in. i.d. tube length was increased to 35 in. Figures 15 and 16 show the results of these two shots. In the propellant confined in the 1.87-in. i.d. tube, detonation failed at about 12 in. whereas the detonation in the larger tube propagated at constant velocity. Figure 15 shows data from both the 20 in. and the 12 in. tests. These data demonstrate that, at least in the case of the M2 propellant, a detonation can be sustained for up to 6 diameters, even when the system is below failure diameter. Figure 17 shows a witness plate from a shot in which a 1.87-in. i.d. copper tube of 6 in. length was loaded with M2 propellant and initiated with PBX 9501. A significant dent in the witness plate resulted from this shot, even though we have demonstrated that the charge was below failure diameter.

Jet Shots

The final test series consisted of firing a small copper jet into a square PMMA box filled with propellant. Shock pins were arranged along the side of the box. Figures 18 (a) and (b) show a static and a dynamic radiograph taken some time later. The jet can be clearly seen. The reaction front appears out in front of the curved jet tip. The object in the upper center of the picture is a pin connector. No dent in the witness plate was observed. However, if the propellant were detonating only at the jet tip (the center region in Figure 1), then the resulting dent could have been swept out by the penetrating jet. The reaction was certainly very violent. During a second shot in this series, a large aluminum x-ray film cassette was thrown nearly 100 ft from the propellant charge. Unfortunately, the film was destroyed.

Conclusions

The following observations and conclusions resulted from the work performed during these initial tests.

(a) The structure at the reaction front was observed by means of radiography. Details of this structure were not clearly identified. Currently, we are digitizing and enhancing several of the radiographs to identify salient features that may help in understanding the failure mechanism.

(b) Detonation velocity is a strong function of confinement.

(c) Detonation velocity is a strong function of charge diameter. This is a good indication that the reaction is not a strong function of the thermodynamic state.

(d) No detonation was observed when the confinement was PMMA.

(e) Failure diameter of the M2 propellant confined in copper is approximately 2 in., and failure can occur up to 6 diameters from the initiating charge.

(f) Several diagnostics have been evaluated and found suitable for this study.

Future work will include a more in-depth examination of the reaction front using radiography as well as ionization pins and possibly manganin gauges to map out pressure histories. The result of this study should be an increased understanding of the initiation and failure of detonations in porous heterogeneous media. We hope to find a relatively simple test that will be able to identify differences in detonability between propellants of varying compositions and structures.

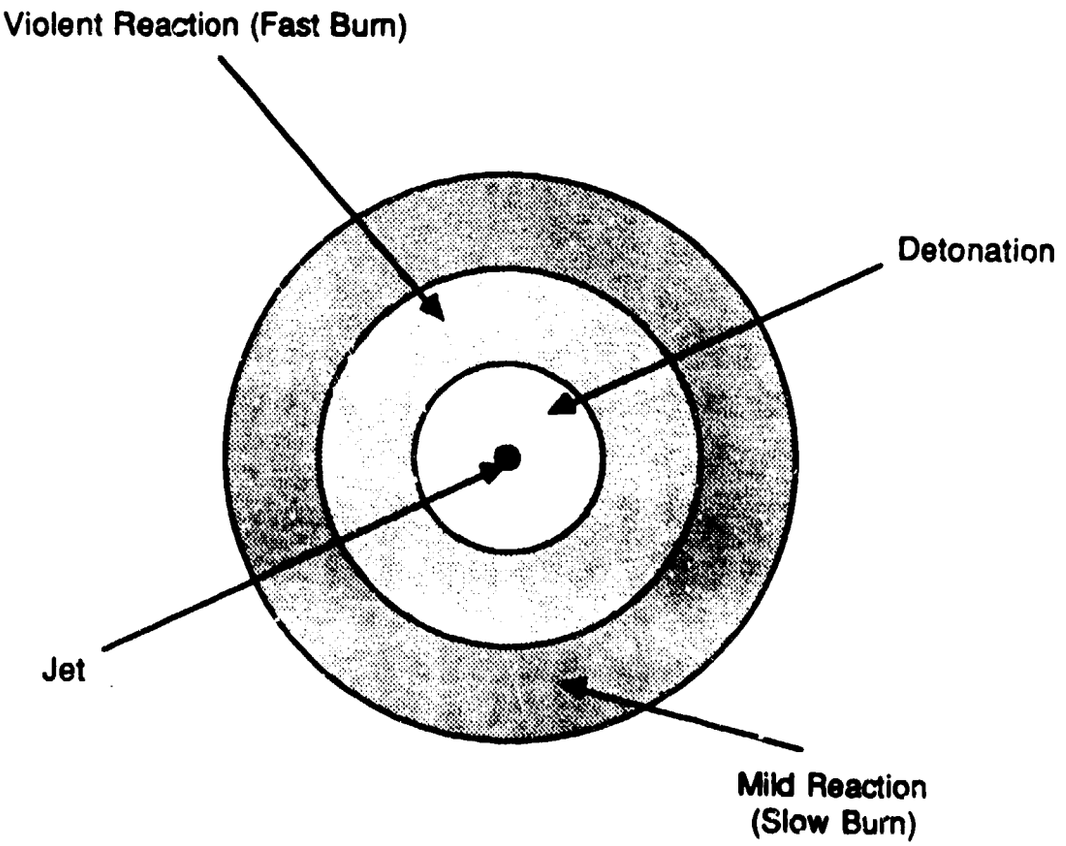

Figure 1. Schematic of regions of interest in the case of detonation failure.

TABLE I

M2 PROPELLANT COMPOSITION AND CHARACTERISTICS

Compound	Composition (wt %)
Nitrocellulose	77.45
Nitroglycerin	19.50
Barium nitrate	1.40
Potassium nitrate	0.75
Graphite	0.30
Ethanol	2.30
Water	0.70

Characteristic	Value
Isochoric Flame Temp (K)	3319
Heat of Explosion (cal/g)	1080
Specific Gravity (g/cm^3)	1.65
Pressure Exponent	0.755

Figure 2. PMMA tube filled with M2 propellant before initiation.

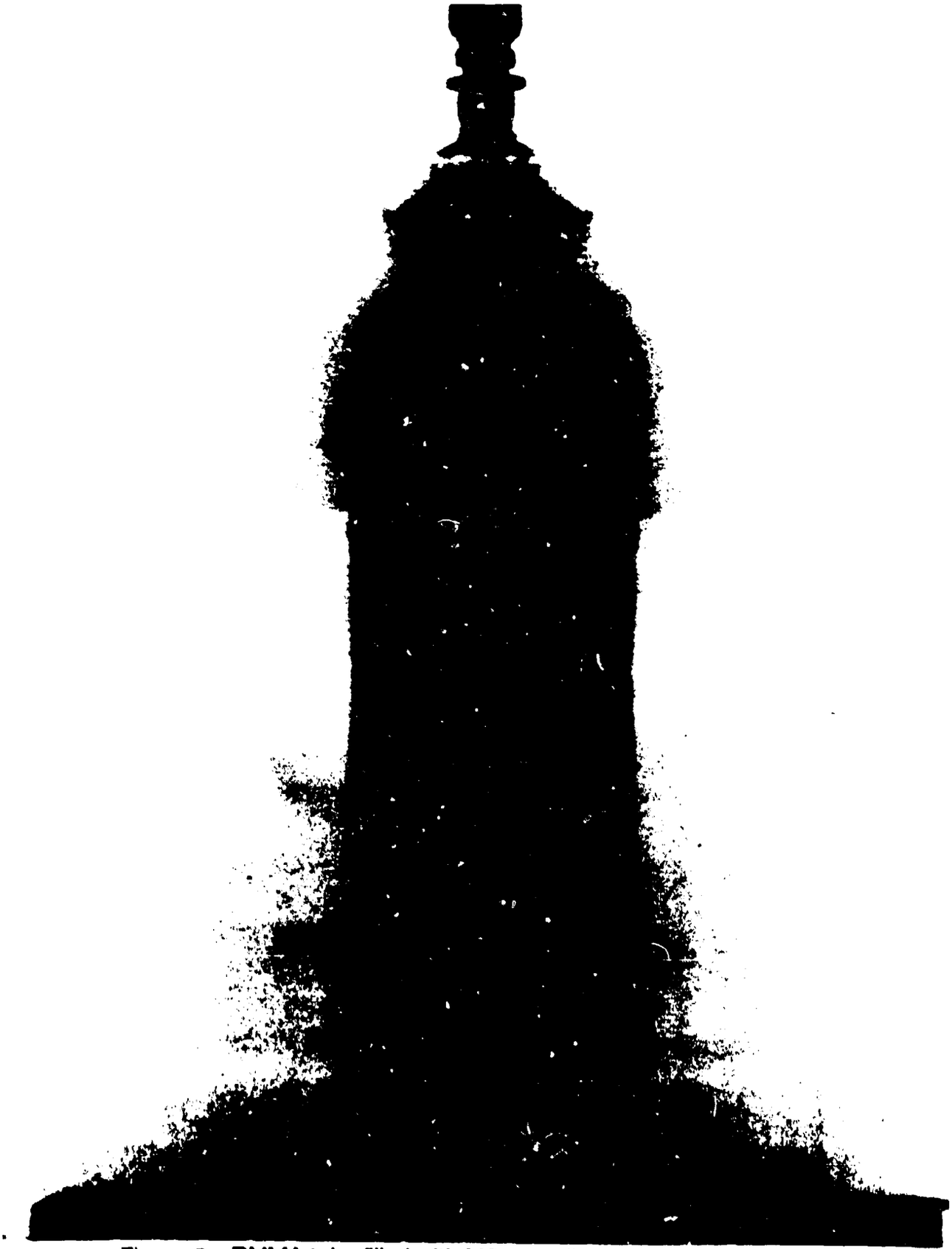

Figure 3. PMMA tube filled with M2 propellant 14 μs after initiation.

Figure 4. PMMA tube filled with M2 propellant 18 μs after initiation.

Figure 5. PMMA tube filled with M2 propellant 27 μs after initiation.

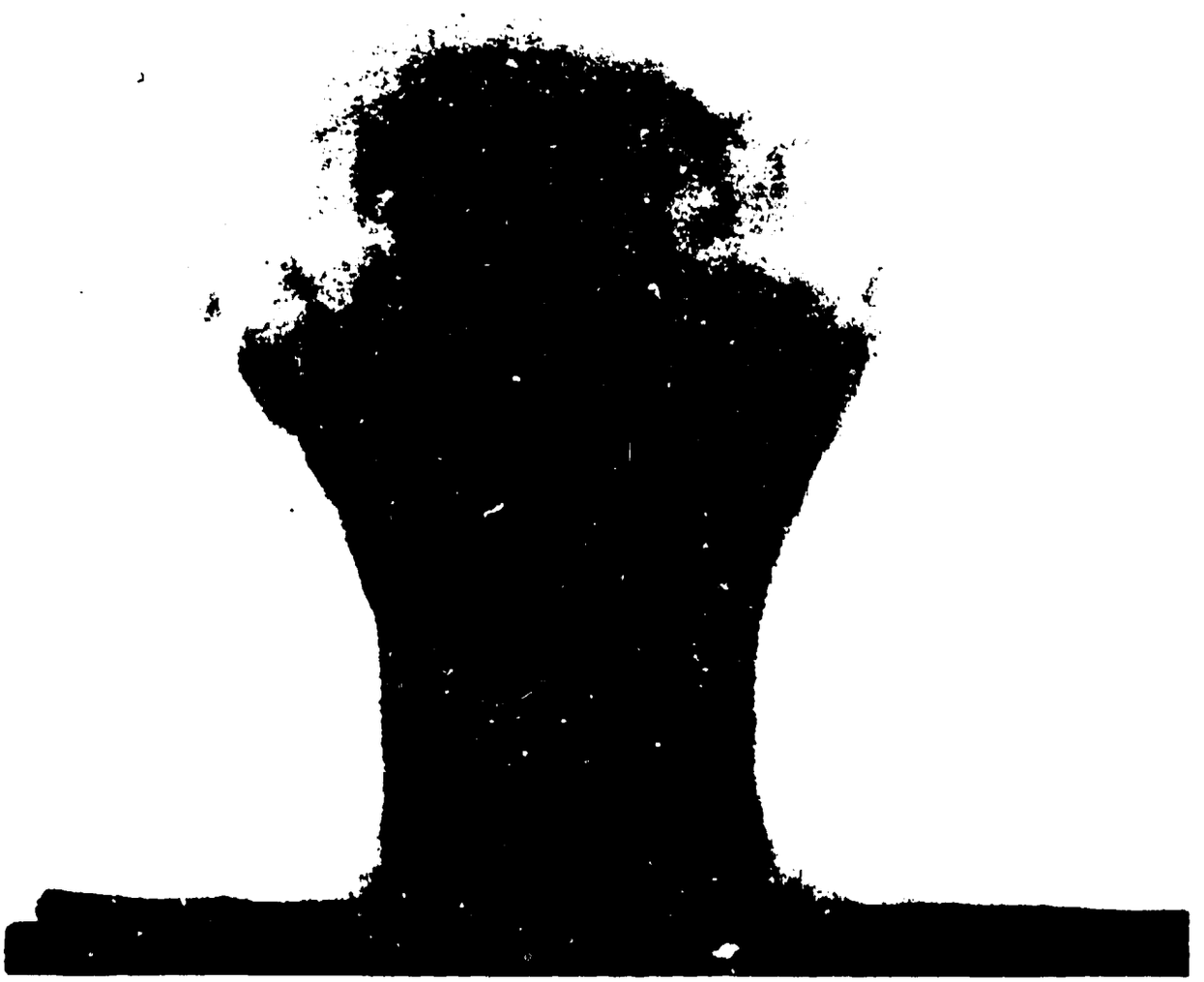

Figure 6. PMMA tube filled with M2 propellant 37 μs after initiation.

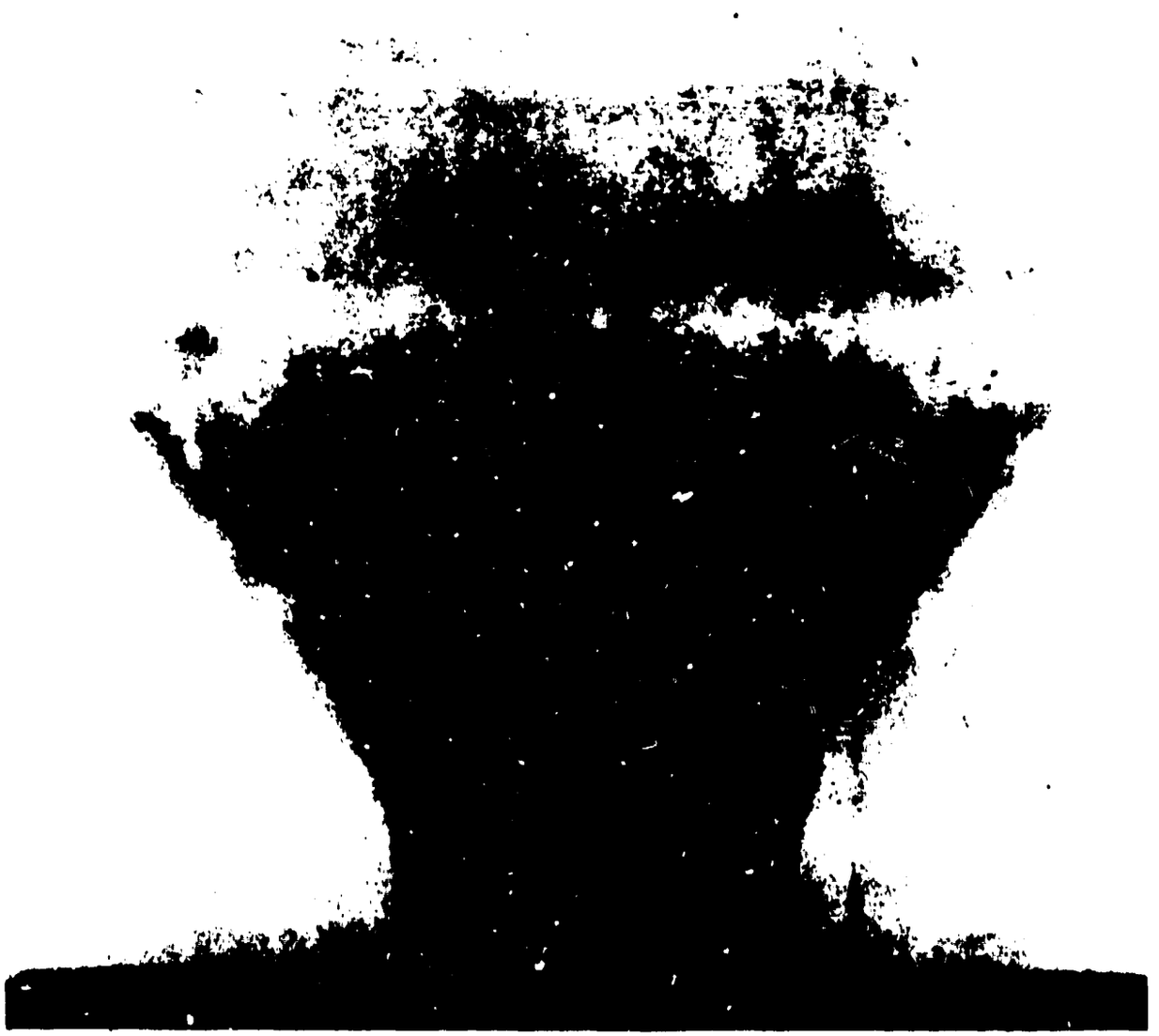

Figure 7. PMMA tube filled with M2 propellant 46 μs after initiation.

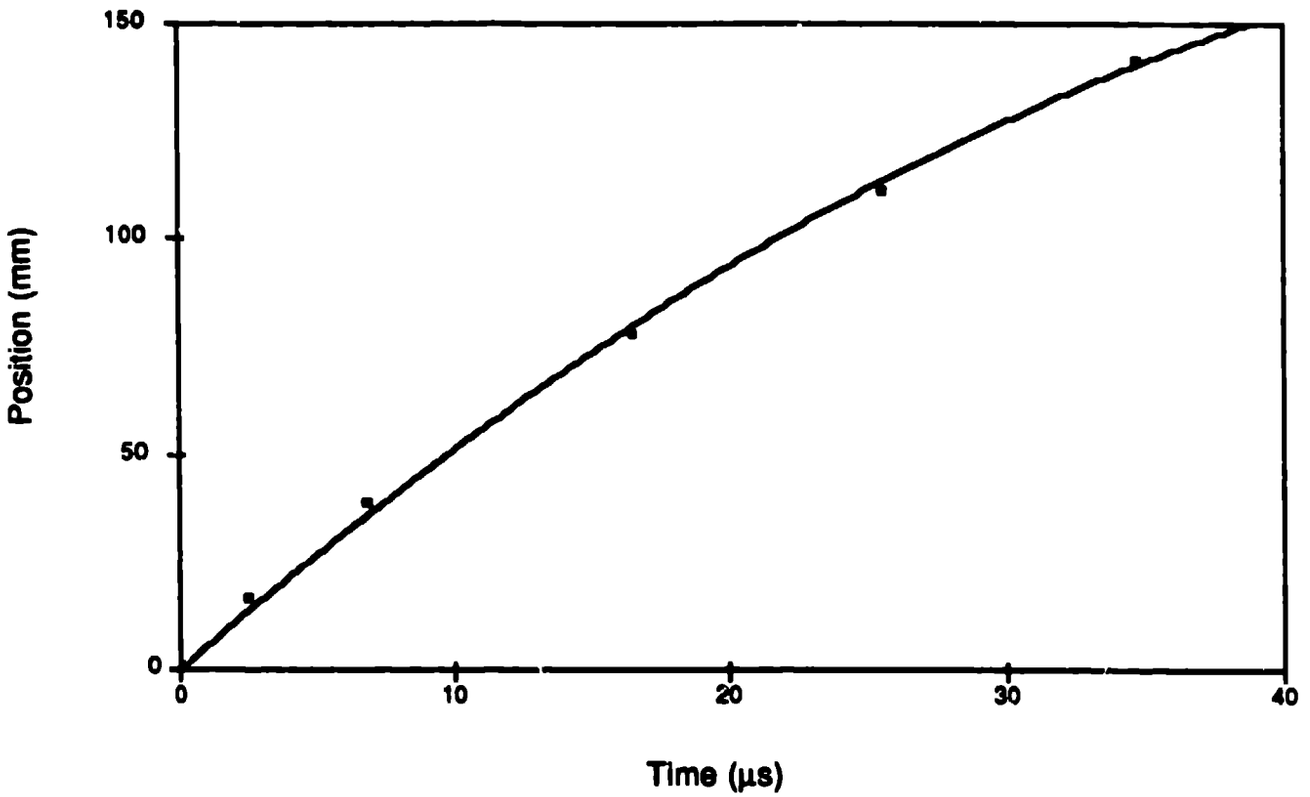

Figure 8. x-t plot of reaction front.

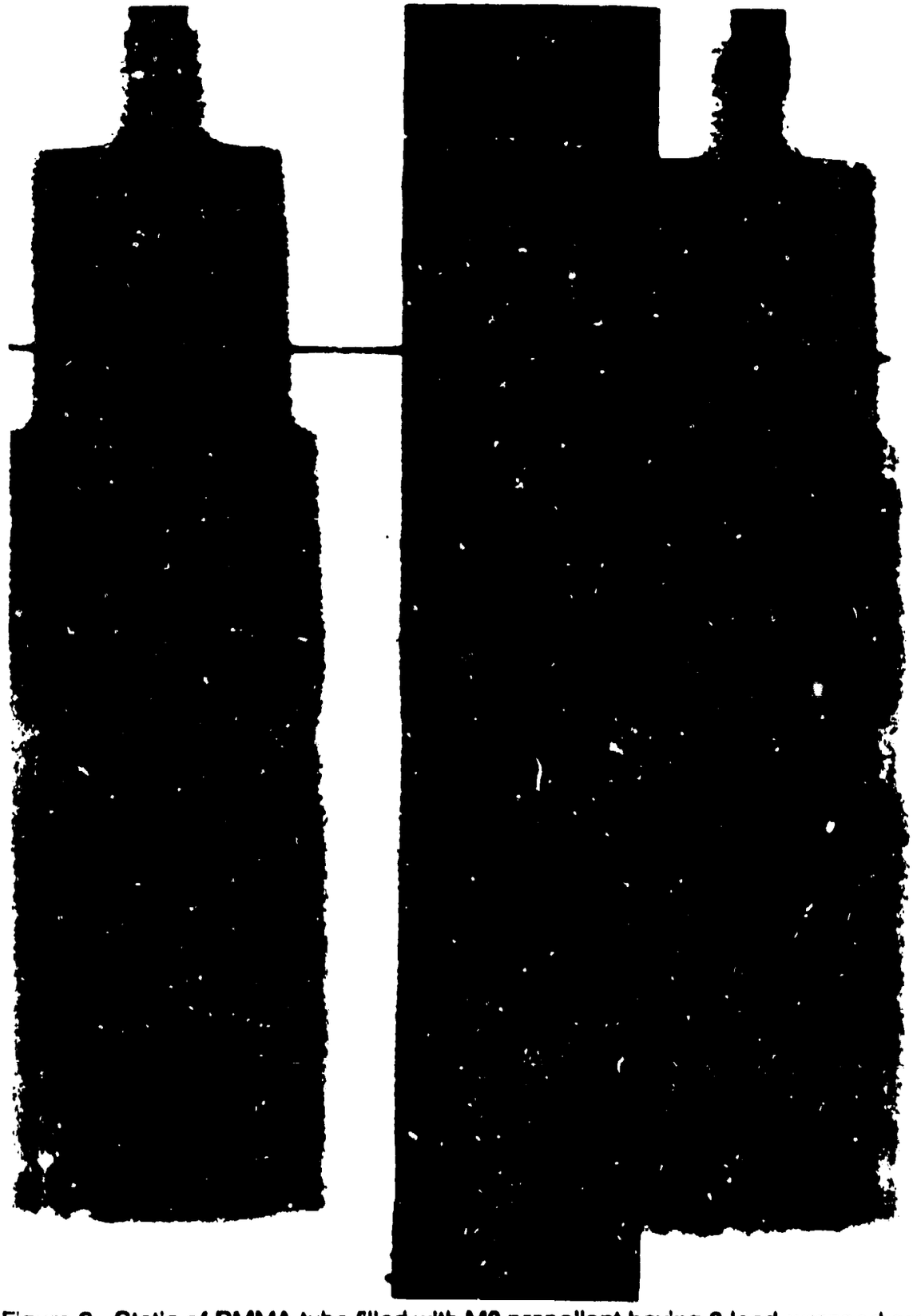

Figure 9. Static of PMMA tube filled with M2 propellant having 3 lead-wrapped grains placed at three locations as tracers.

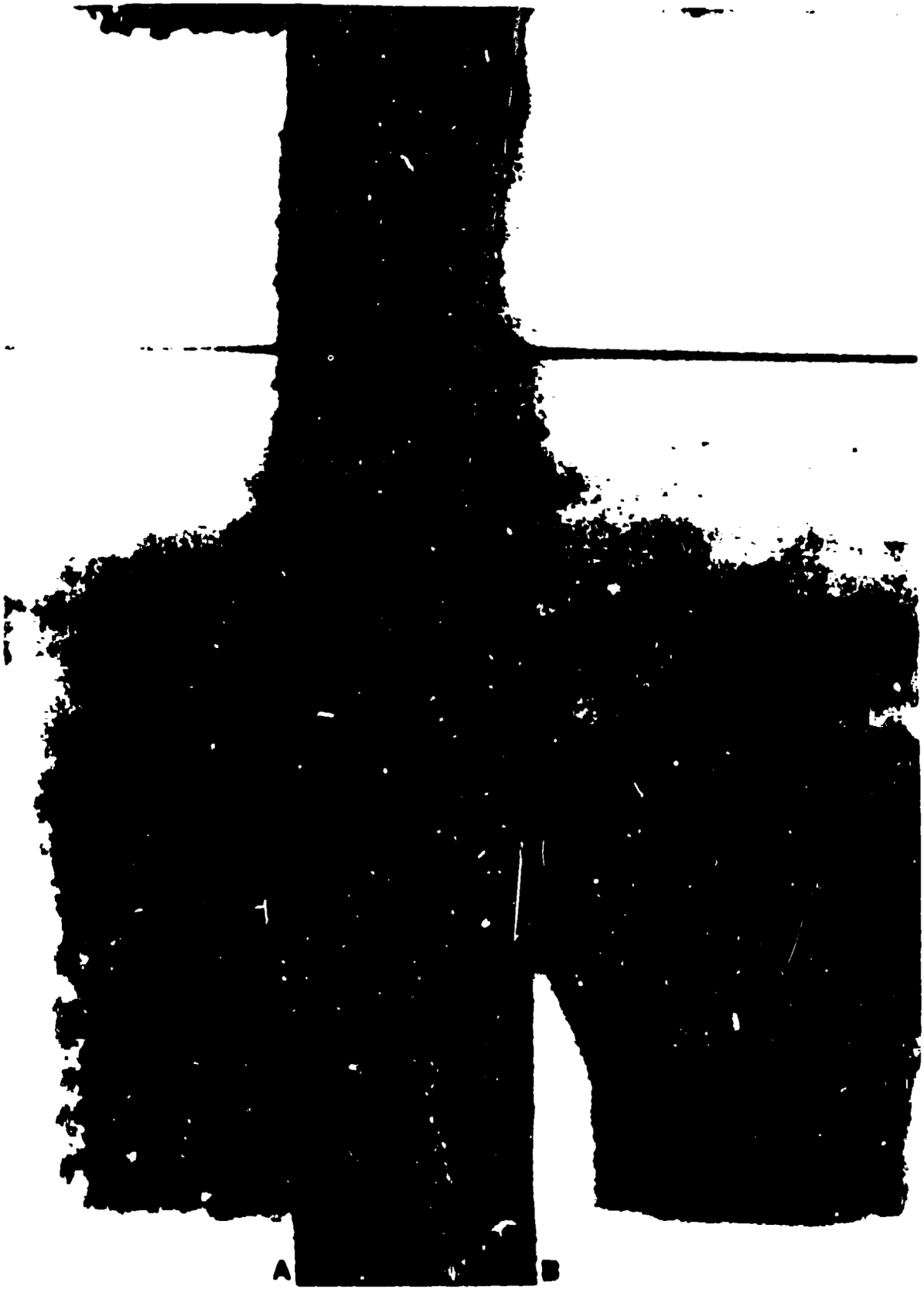

Figure 10. Xrays taken at two times of PMMA tube containing tracer grains. Wave motion is from top to bottom.

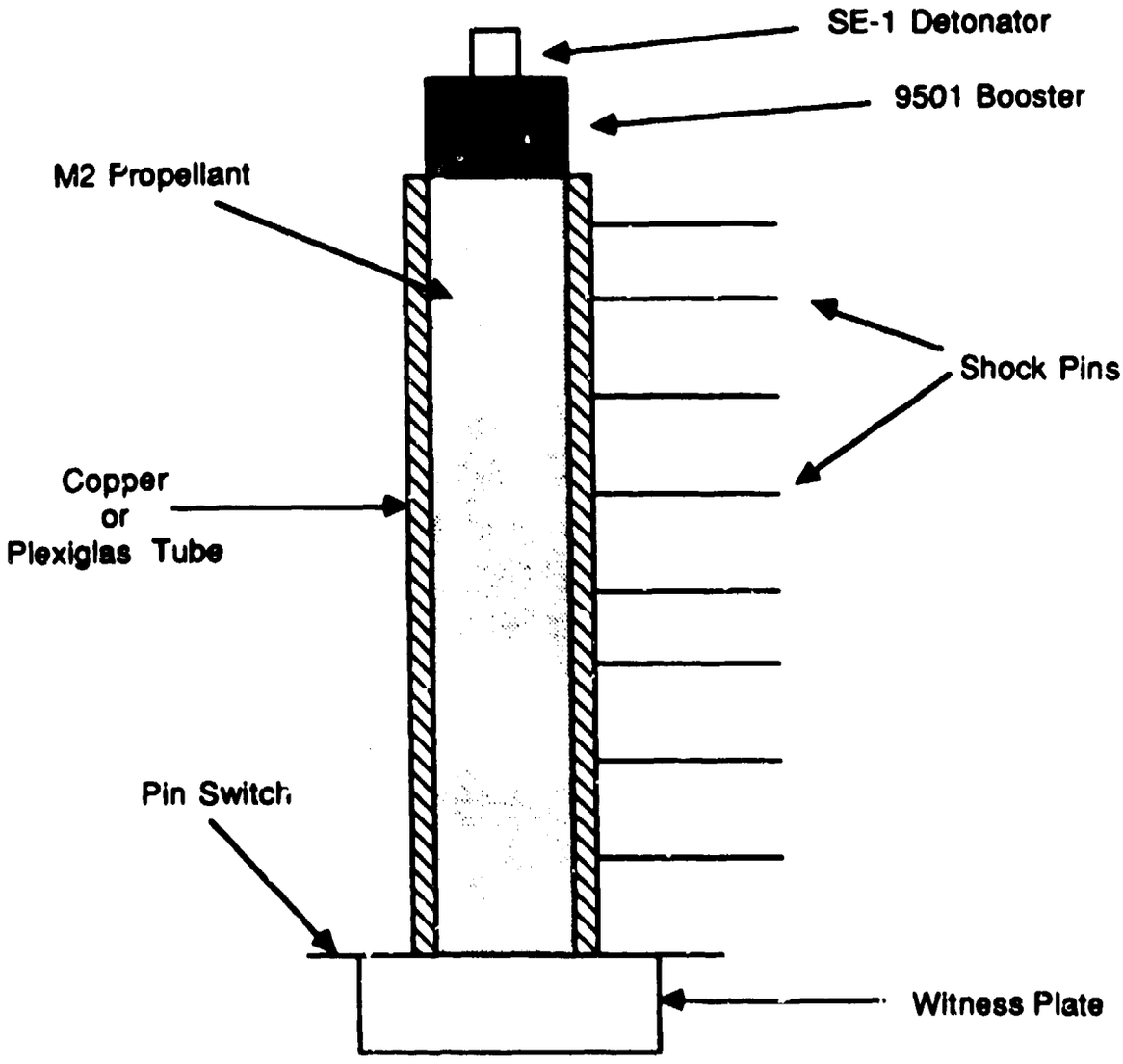

Figure 11. Schematic of test configuration for instrumented pin shots.

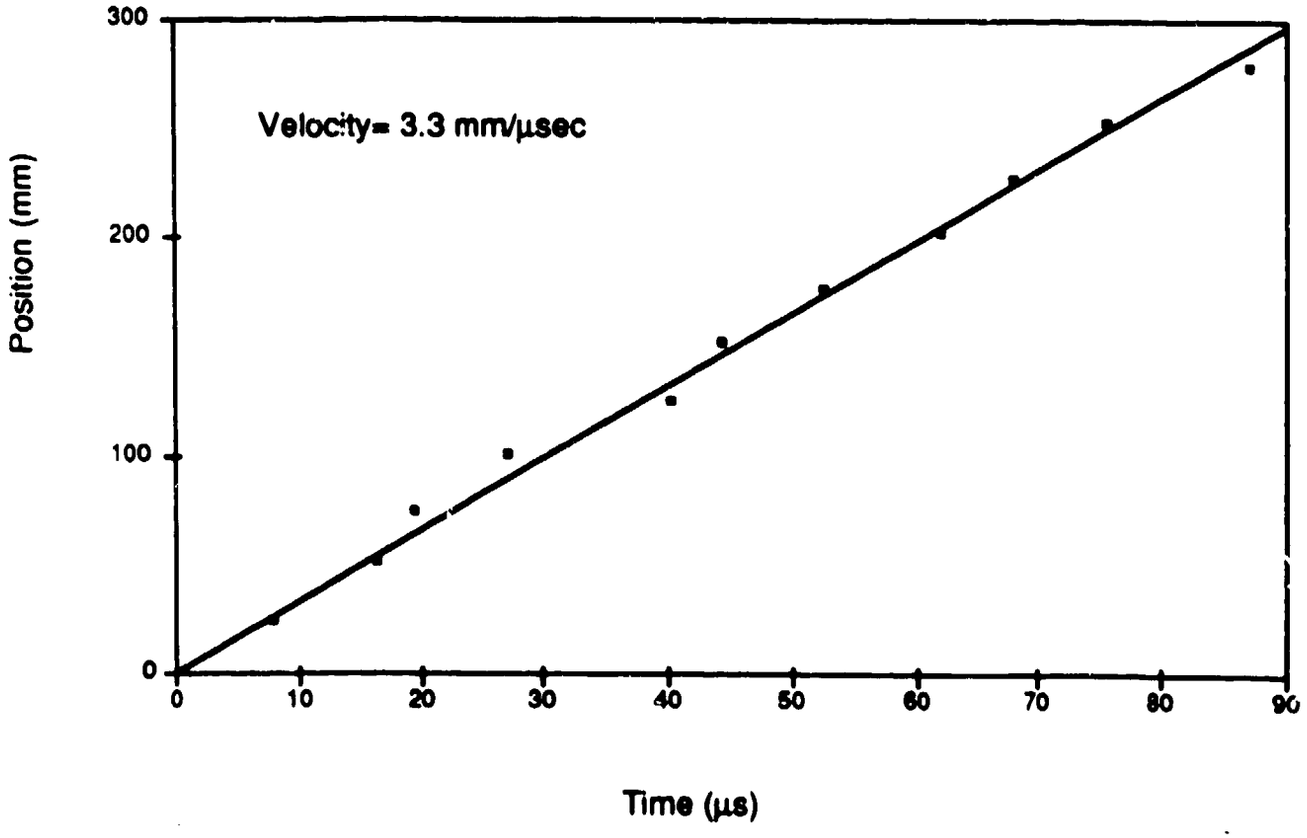

Figure 12. x-t plot for Shot No. C5851.

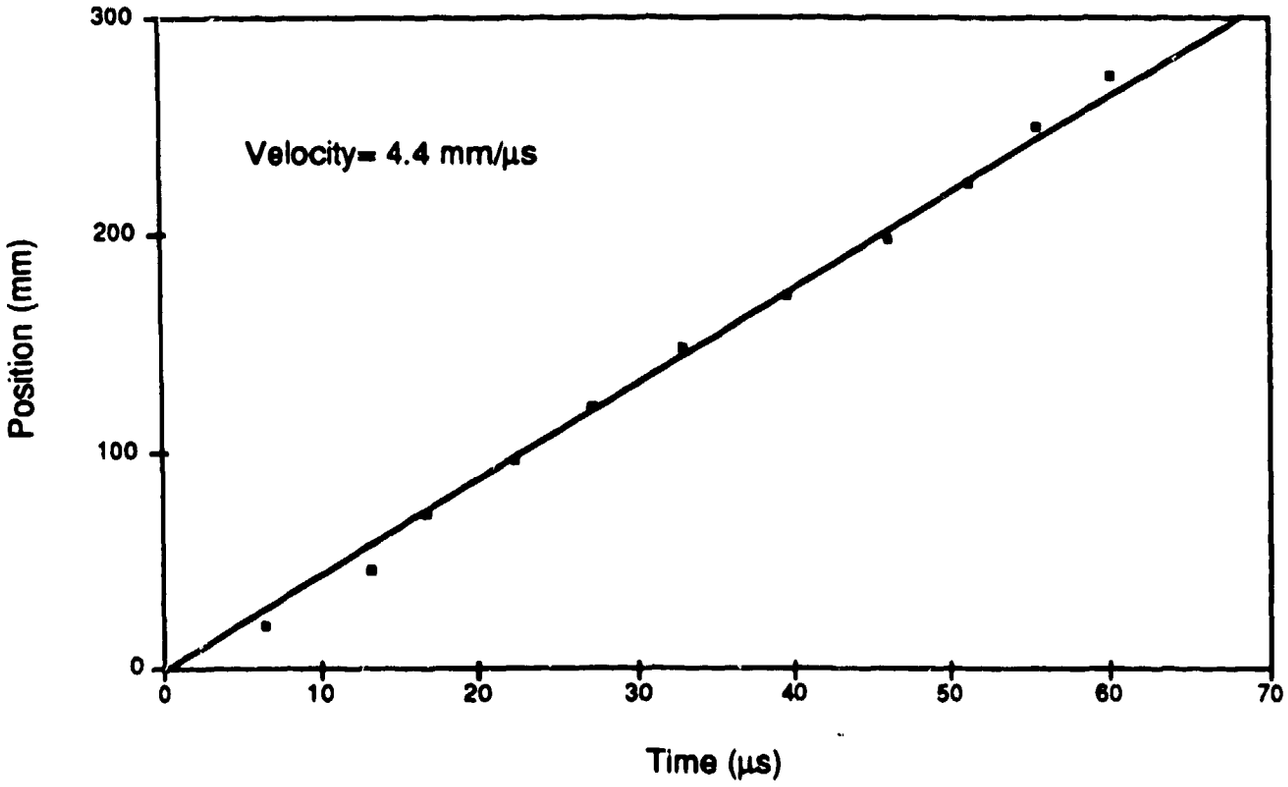

Figure 13. x-t plot for Shot No. C5855.

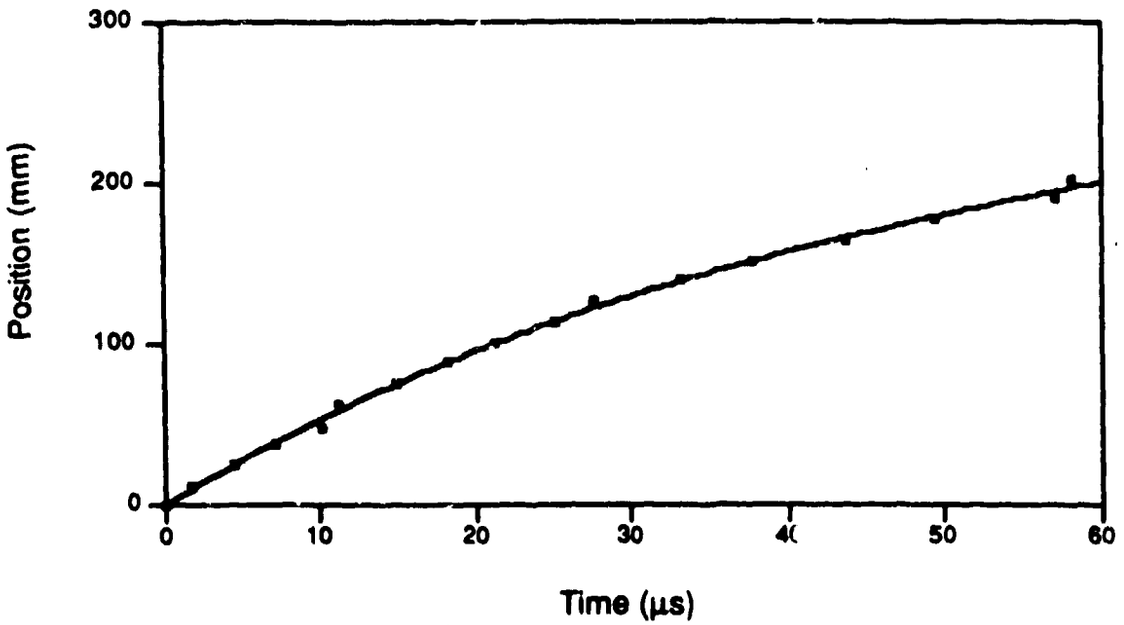

Figure 14. x-t plot for Shot No. C5856

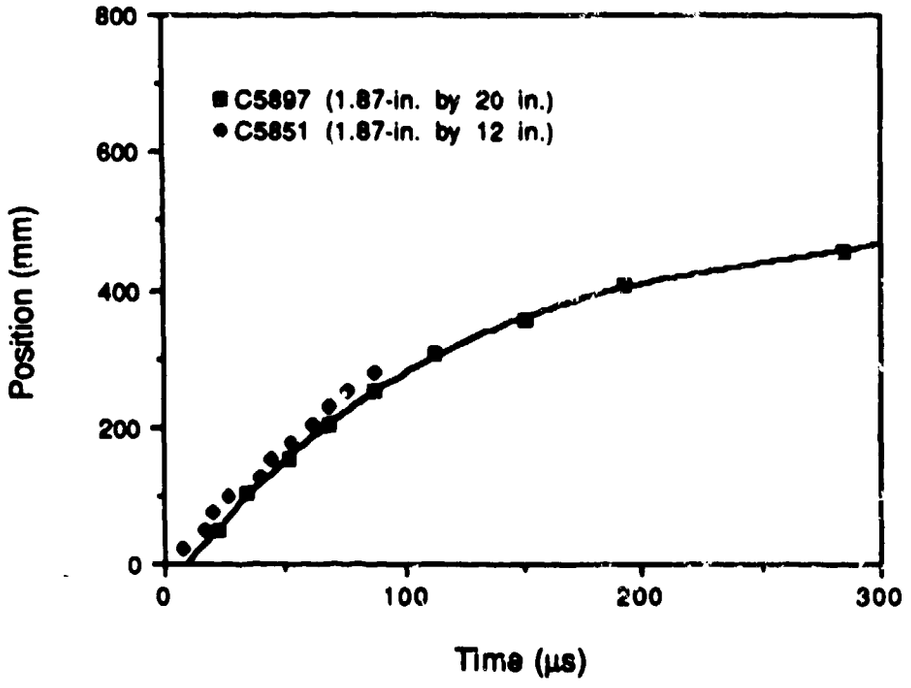

Figure 15. Comparison of data from tubes 1.87-in. i.d. and 12 in. and 20 in. long- M2 propellant

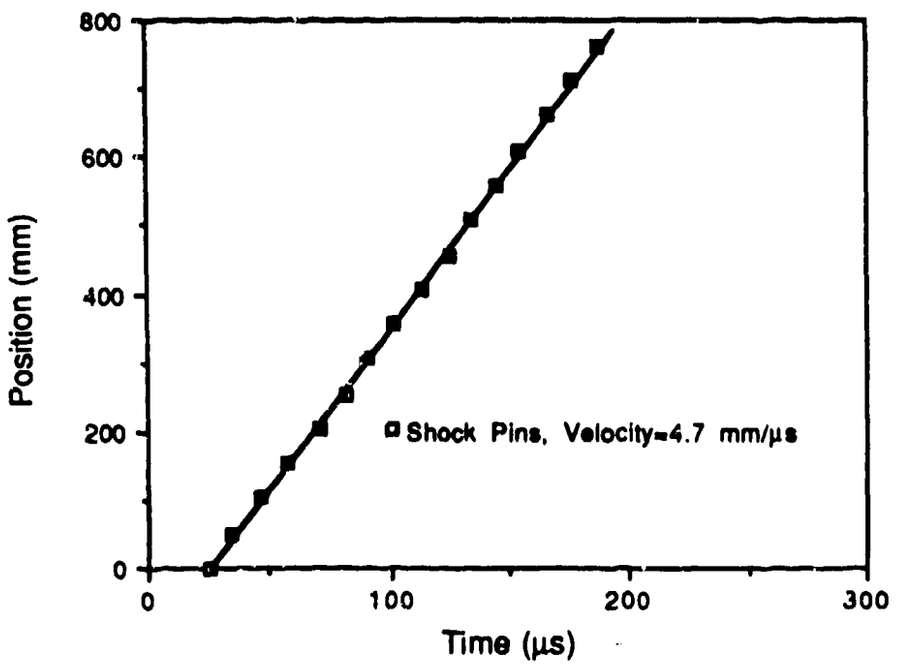

Figure 16. Shock pin data from 2.87- by 35 in. tube (Shot No. C5898)-M2 propellant.

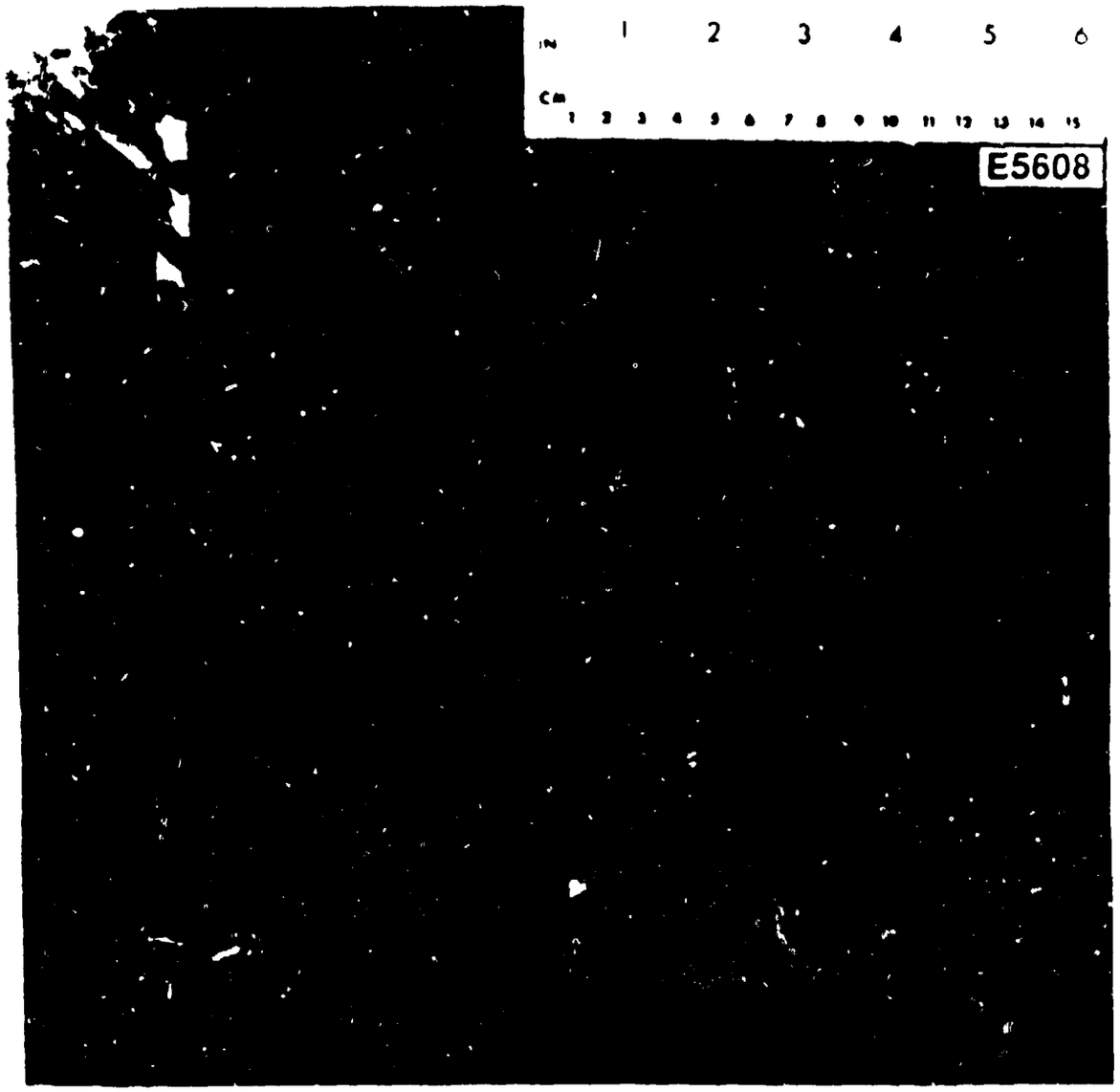

Figure 17. Steel witness plate from Shot No. E5608.

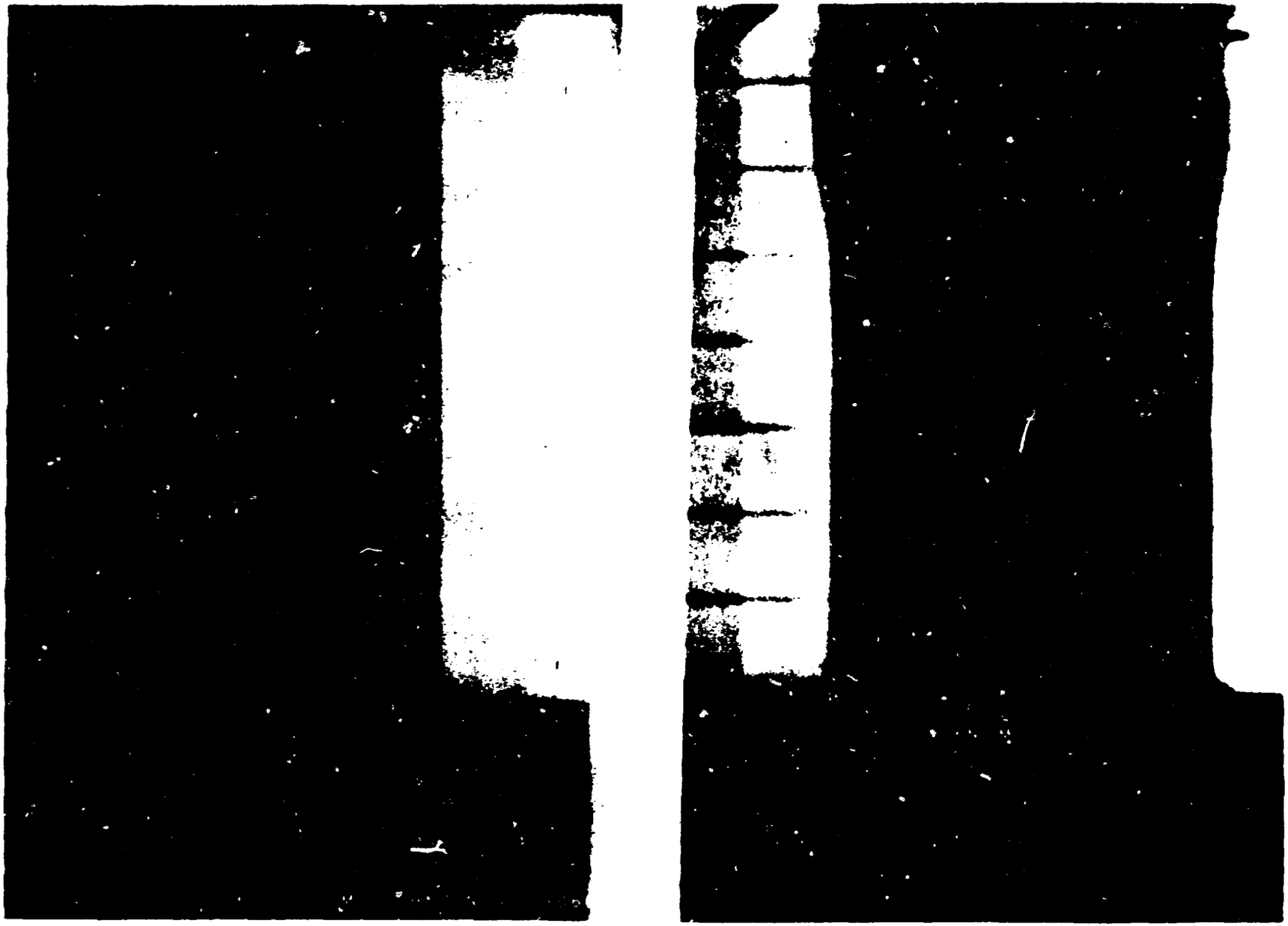

Figure 18. Static (a) and dynamic (b) of copper jet penetrating PMMA box filled with M2 propellant .